

# Apparent Directional Emittances of Random Rough Surfaces of Metals and Nonmetals\*

by Kimio KANAYAMA\*\*

(Received September 30, 1971)

It is a well-known fact that the graphic forms of the apparent directional emittances of the metallic and the nonmetallic rough surfaces, indicated in polar co-ordinates, are different from those of the flat smooth surfaces of the same kinds.

A theoretical analysis of the apparent directional emittances of the metallic and the nonmetallic random rough surfaces was performed, assuming the roughness of those surfaces was composed of various sorts of circular arc grooves distributed regularly at a fixed rate. The apparent directional emittances were calculated applying the emissive characteristics given by the approximate formula introduced by E. Schmidt and other for metals and applying Fresnel's formula for nonmetals to the inside surface of the groove. The apparent directional emittances of the metallic rough surfaces of aluminum and brass scratched with various grain sized sandpapers and the nonmetallic rough surfaces coated with the asbestos mixture paints were measured, and the result of the theoretical analysis was compared with the experimental result.

## 1. Introduction

In general, it is already made clear that the normal emissivity of the metallic flat surface is of small value, the directional emissivity indicated in polar co-ordinates increases in proportion as a directional angle measured from the normal to the plane of specimen increases, and the tendency of increment agrees well with the theoretical formula introduced by Schmidt and other<sup>1)</sup>. Also, when a metallic flat surface is adequately roughened by any means, the normal emittance of the rough surface is usually greater than that of the flat surface and the graphic form of the directional emittance is changed<sup>2)</sup>.

On the other hand, the directional emissivity of a nonmetallic flat surface is of a nearly constant large value in a region of the directional angle about  $0\sim 45^\circ$ , and decreases steeply in proportion to the increment of the directional angle and is zero at a directional angle of  $90^\circ$ . The absolute value and the tendency of the directional emissivity agree well with Fresnel's formula on a nonmetallic flat surface. In many cases, however, the nonmetallic surface has an appropriate roughness, and the graphic form of the apparent directional emittance on such rough surface is also changed<sup>3)</sup>.

In this study, these roughened surfaces are tentatively named the random rough surfaces, on the apparent directional emittances of these surfaces are performed theoretical analyses, supposing that the surface irregularity is shaped

\* Translation into English of a paper contributed to Trans. JSME.

\*\* Department of Mechanical Engineering, Kitami Institute of Technology.

in the circular arc groove and the random rough surfaces are composed of various sorts of these grooves distributed in any fixed rate. At the same time, on the metallic materials, such as the aluminum and the brass rough surfaces scratched with the various grain-sized sandpapers and on the nonmetallic materials, such as the paint rough surfaces coated with the asbestos tailing mixture heat resisting paints, the apparent directional emittances are measured and the analytical results are experimentally proved.

### 2. Theoretical Analysis

The theoretical analysis is performed, supposing the dimension of the opening of the circular arc groove which composes the rough surface is larger than wavelength of the emission, in the relation between the incidence and the reflection of emission beam on the inside surface of groove is kept the geometrical optics, furthermore, the analysis is made two-dimensionally.

#### 2.1 Basic Formula of Apparent Directional Emittance

Co-ordinates and symbols are shown in Fig. 1 with which the apparent directional emittance on an opening of groove is calculated. The basic formula of the apparent directional emittance  $\epsilon_{a\phi}$ , in direction  $\phi$  measured from the normal of the opening of groove, is

$$\epsilon_{a\phi} = \frac{1}{2} \left( \frac{1}{\cos \phi \cos \gamma} \sum_1^i \left[ \left\{ 1 - (1 - \epsilon_{\varphi_i})^\xi \right\} \left\{ \sin(\varphi_i)_f - \sin(\varphi_{i-1})_f \right\} \right] + \frac{1}{\cos \phi \cos \gamma} \sum_1^i \left[ \left\{ 1 - (1 - \epsilon_{\varphi_i})^\xi \right\} \left\{ \sin(\varphi_i)_n - \sin(\varphi_{i-1})_n \right\} \right] \right), \quad (1)$$

where

$$\left. \begin{aligned} (\varphi_i)_f &= \frac{\pi}{2} \cdot \frac{2i - \left(1 + \frac{2\phi}{\pi}\right) + \frac{2\gamma}{\pi}}{2i + 1} \leq \frac{\pi}{2} - (\phi + \gamma) \\ (\varphi_i)_n &= \frac{\pi}{2} \cdot \frac{2i - \left(1 - \frac{2\phi}{\pi}\right) + \frac{2\gamma}{\pi}}{2i + 1} \leq \frac{\pi}{2} - |\phi - \gamma| \end{aligned} \right\} \quad (2)$$

at  $i=0$ , in general  $(\varphi_0)_f = (\varphi_0)_n = 0$ ,

when  $\phi > \frac{\pi}{2} - \gamma$ ,  $(\varphi_0)_n = \phi - \left(\frac{\pi}{2} - \gamma\right)$

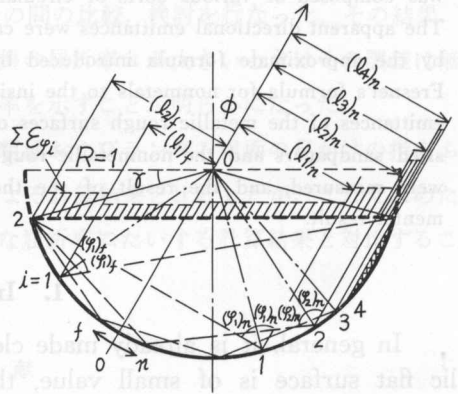


Fig. 1. Co-ordinates and symbols of circular arc groove model.

The first term of Eq. (1) indicates the apparent directional emittance on the far wall looked from the direction of the emission, the second term indicates

that on the near wall and these are distinguished by using suffixes  $f$  and  $n$  respectively.

**2.2 Apparent Directional Emittance of Metallic Random Rough Surface**

The specific emissivity of the metallic flat surface  $\epsilon_\varphi$  is approximately indicated as<sup>4)</sup>

$$\epsilon_\varphi = \frac{1}{n} \left( \cos \varphi + \frac{1}{\cos \varphi} \right), \tag{3}$$

where  $n$ =refraction index,  $\varphi$ =directional angle,  $0^\circ \leq \varphi < 90^\circ$ .

The specific average emissivity  $\epsilon_{\varphi_i}$ , on a surface element which emits the reflection components of same number of reflections  $(i-1)$  on the inside surface of the circular arc groove, is

$$\epsilon_{\varphi_i} = \frac{\int_{\varphi_{i-1}}^{\varphi_i} \epsilon_\varphi \cdot d\varphi}{\int_{\varphi_{i-1}}^{\varphi_i} d\varphi} \tag{4}$$

Substituting Eq. (3) into Eq. (4) yields

$$\begin{aligned} \epsilon_{\varphi_i} &= \frac{\frac{1}{n} \cdot \int_{\varphi_{i-1}}^{\varphi_i} \left( \cos \varphi + \frac{1}{\cos \varphi} \right) d\varphi}{\int_{\varphi_{i-1}}^{\varphi_i} d\varphi} \\ &= \frac{\frac{1}{n} \cdot \left[ \sin \varphi + \log_e \tan \left( \frac{\varphi}{2} + \frac{\pi}{4} \right) \right]_{\varphi_{i-1}}^{\varphi_i}}{\varphi_i - \varphi_{i-1}} \end{aligned} \tag{4'}$$

The sum total of the average emissivity  $\sum \epsilon_{\varphi_i}$ , which consists of the reflection components of maximum number of reflections  $(i-1)$  on the element of the average emissivity  $\epsilon_{\varphi_i}$ , is indicated by the following polynomial equation

$$\begin{aligned} \sum \epsilon_{\varphi_i} &= \left\{ \epsilon_{\varphi_i} + (1 - \epsilon_{\varphi_i}) \epsilon_{\varphi_i} + (1 - \epsilon_{\varphi_i})^2 \epsilon_{\varphi_i} + \dots + (1 - \epsilon_{\varphi_i})^{i-1} \epsilon_{\varphi_i} \right\} \\ &= 1 - (1 - \epsilon_{\varphi_i})^i \end{aligned} \tag{5}$$

In Eq. (5), the first term is a component of direct emission, the second term is a component of reflection number one, the third term is a component of reflection number two, ...,  $i$ -th term is a component of reflection number  $(i-1)$ .

Substituting into Eq. (1)  $\sum \epsilon_{\varphi_i}$  obtained by substituting Eq. (4') into Eq. (5) and applying the conditional equation (2), the apparent directional emittance concerning a circular arc groove is calculated. On the calculations, with respect to each value of the refraction index  $n=90, 70, 50, 30, 20$  and  $15$ , the combinations of the deflection angle  $\gamma$  and the directional angle  $\phi=0^\circ, 15^\circ, 30^\circ, 45^\circ, 60^\circ, 75^\circ$  and  $90^\circ$  are used as parameters respectively. When the calculation of Eq. (5) are carried out, guessing from the results of comparison between the

calculated values and the measured data on the published paper<sup>5)</sup>, the calculation for the surface element of  $i > 3$  is put an end up to  $i = 3$ , that is, the sum total of the reflection components is up to reflection number  $(i - 1) = 2$ .

In the next place, it is assumed that the random rough surfaces composed of the circular arc groove consist of seven sorts of the circular arc grooves  $\gamma = 0^\circ, 15^\circ, 30^\circ, 45^\circ, 60^\circ, 75^\circ$  and  $90^\circ$  (flat surface) and that each sort of the grooves distributes regularly in an average value of 0, a measure of dispersion of  $1^{(6),(7)}$ . Namely, the probability density  $P(\xi)$  for a variable  $\xi$  is

$$P(\xi) = \frac{1}{\sqrt{2\pi}} e^{-\frac{\xi^2}{2}}. \quad (6)$$

Where, by means of that  $\gamma = 30^\circ$  corresponds to  $\xi = 1.0$ , the calculation of the  $P(\xi)$  for each  $\gamma$  is performed, and furthermore, by redistributing proportionally the calculated value according to a rate at which the sum of the  $P(\xi)$  equals unity, the distribution weight  $w_\gamma$  for each  $\gamma$  is obtained. The calculated results of the distribution weight  $w_\gamma$  are shown in Fig. 2. In Fig. 2, the distribution curve whose the maximum distribution weight corresponds to  $\gamma$  is indicated by the symbol of  $\hat{\gamma}$ .

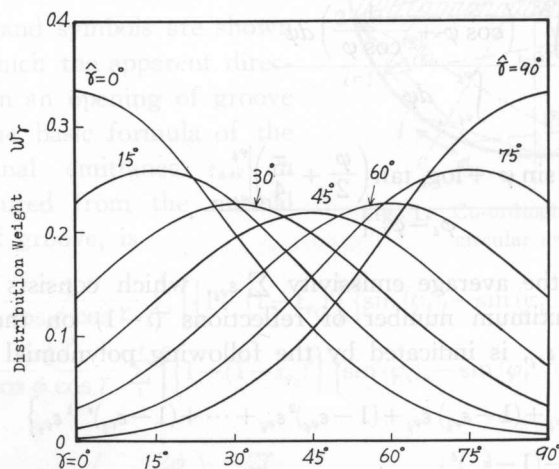


Fig. 2. Distribution weights of various sorts of the circular arc grooves.

The apparent directional emittance of the random rough surface composed of various sorts of the circular arc grooves is obtained, by summing up the products of the directional emittances and the distribution weights for each  $\gamma$ . The calculated results of the apparent directional emittances in case refraction index  $n = 90, 70, 50, 30, 20$  and  $15$ , moreover, containing a flat surface, are shown in Fig. 3. It means that, according as the value of  $\hat{\gamma}$  transfers from  $90^\circ$  to  $0^\circ$  on each index  $n$ , the distribution rate of the deep groove increases. In this place, it is clear that the directional characteristics of the metallic flat surface is bereft of, the emittance increases in normal direction to the specimen

surface and decreases excessively in large directional angle. In the case of  $\hat{\gamma}=45^\circ$  or  $30^\circ$ , the apparent directional emittances are nearly constant out of relation to the directional and the forms of graphic curves approach the semi-circular shapes.

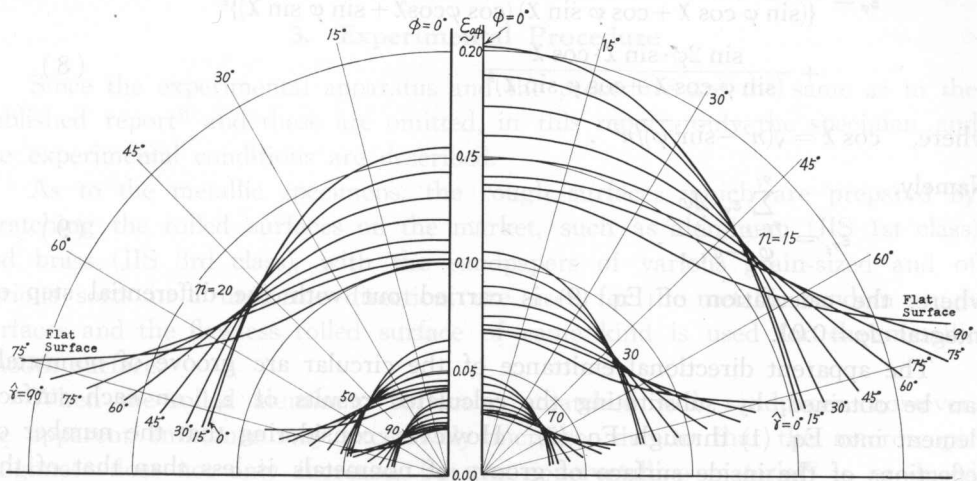


Fig. 3. Apparent directional emittances of the metallic random rough surfaces composed of various circular arc grooves (calculated values).

### 2.3 Apparent Directional Emittance of Nonmetallic Random Rough Surface

The analytical procedure in nonmetallic materials is in the same manner as in case of the metallic materials. In the first place, the apparent directional emittances of the opening composed of a sort of circular arc groove for each  $\hat{\gamma}$  are computed, supposing that the directional characteristics of the inside surface of groove for the emission and for the reflection of radiation beam are given by Fresnel's formula concerning the nonmetallic flat surface.

The general form of Fresnel's formula, which gives the directional emissivity, is

$$\epsilon_\varphi = \frac{1}{2} \left\{ \frac{\sin 2\varphi \cdot \sin 2\chi}{\sin^2(\varphi + \chi) \cdot \cos^2(\varphi - \chi)} + \frac{\sin 2\varphi \cdot \sin 2\chi}{\sin^2(\varphi + \chi)} \right\}. \tag{7}$$

In Eq. (7), the first term is a component vibrating parallel to the incident plane, the second term a perpendicular component. Here, Snell's law  $\sin \varphi = n \sin \chi$  comes into existence in relation between an emission angle  $\varphi$  and an incidence angle  $\chi$  interior of the solid.

The specific average emissivity  $\epsilon_{\varphi_z}$  on an element of inside surface of the circular arc groove, which consists of the same number of reflections, is obtained by substituting Eq. (7) into Eq. (4), but by the reason for the difficulty of integration of Eq. (7),  $\epsilon_{\varphi_z}$  can be approximately computed by means of the numerical integration.

After Eq. (7) is transformed into Eq. (8) in order to simplify the numerical calculation, substituting this into Eq. (9),  $\epsilon_{\varphi_i}$  is computed by the aid of an electronic computer (JEOL JEC-5).

$$\epsilon_{\varphi} = \frac{2 \sin 2\varphi \cdot \sin \chi \cdot \cos \chi}{\{(\sin \varphi \cos \chi + \cos \varphi \sin \chi) (\cos \varphi \cos \chi + \sin \varphi \sin \chi)\}^2} + \frac{\sin 2\varphi \cdot \sin \chi \cdot \cos \chi}{(\sin \varphi \cos \chi + \cos \varphi \sin \chi)^2} \quad (8)$$

where,  $\cos \chi = \sqrt{(n^2 - \sin^2 \varphi) / n^2}$ .

Namely,

$$\epsilon_{\varphi_i} = \frac{\sum_{\varphi_{i-1}}^{\varphi_i} \epsilon_{\varphi} \cdot \Delta\varphi}{\varphi_i - \varphi_{i-1}}, \quad (9)$$

where, the calculation of Eq. (9) is carried out with the differential step of integral  $\Delta\varphi = 0.01$ .

The apparent directional emittance of the circular arc groove of nonmetals can be obtained, by substituting the calculated results of  $\epsilon_{\varphi_i}$  on each surface element into Eq. (1) through Eq. (5). However, considering that the number of reflections of the inside surface of groove of nonmetals is less than that of the metallic surface, the calculation for the surface element of  $i > 2$  is put an end up to  $i = 2$ , namely, sum of the reflection number  $(i - 1) = 1$ .

The calculating procedure of the apparent directional emittance on the nonmetallic random rough surfaces is the same as in the case of metals. The calculated values of the apparent directional emittances in case  $n = 1.25, 1.50, 1.75$  and  $2.00$ , containing the result of the flat surface, are shown in Fig. 4. In the figure, according to the transfer from  $\hat{r} = 90^\circ$  to  $0^\circ$ , the distribution rate of the deep groove increases and the values of the apparent directional emittance

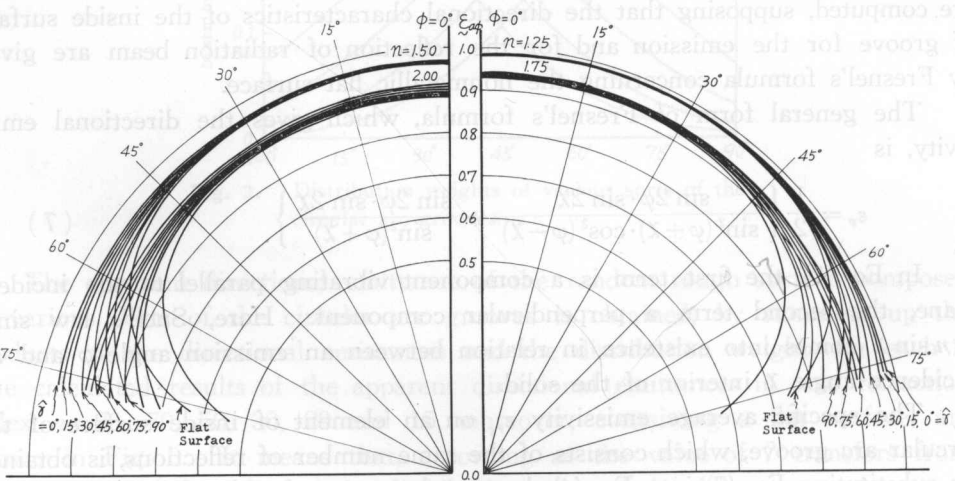


Fig. 4. Apparent directional emittances of the nonmetallic random rough surfaces composed of various circular arc grooves (calculated values).

increase, and moreover, its increment rate appears particularly in a large directional angle. As a result, the graphic form of the emittance approaches nearly the semi-circular shape, and it seems that the diffused surface is created to which Lambert's law can almost be applied.

### 3. Experimental Procedure

Since the experimental apparatus and the procedure are the same as in the published report<sup>5)</sup> and these are omitted, in this report, only the specimen and the experimental conditions are described.

As to the metallic specimens, the rough surfaces which are prepared by scratching the rolled surfaces on the market, such as aluminum (JIS 1st class) and brass (JIS 3rd class), with the sandpapers of various grain-sized and of various sorts in a uniform direction, are used for the metallic random rough surfaces and the flawless rolled surface of same kind is used for the metallic smooth surface.

When the rolled aluminum surface is scratched with sandpaper, however, the apparent emittance may excessively increase, due to that the macroscopic roughness does not only increase, but the noncrystalline material<sup>8)</sup> is produced on the aluminum surface in case of scratching with the grain of sandpaper and but the heterogeneous material is produced by the mutual reaction among a roll-skin formed in case of the roll working of aluminum, a grain of sandpaper and a binding agent.

To remove the effects of "contaminations" on the aluminum rough surface, by creating the vacuum deposit film ( $0.5\sim 1.0\ \mu$ ) over that surface, the surfaces prepared as purely as possible are used for specimens. On the brass surface, as the contaminations by scratching are scarcely produced, the scratched surfaces are used in that condition.

The measurements on the metallic specimens were performed on the experimental conditions that temperature of the specimen was  $200^{\circ}\text{C}\pm 1\%$ , temperature of the black body  $200^{\circ}\text{C}\pm 0.5\%$ , room temperature  $20\sim 21^{\circ}\text{C}$  and relative humidity below 35%.

As to the nonmetallic specimens, the painting surfaces coated with heat resisting paints on the aluminum plates are used for the flat smooth surfaces and the painting surfaces coated with asbestos tailing mixture paints in a mixing rate of paint : asbestos = 3 : 2 in weight, are used for the random rough surfaces. The heat resisting paint is "Pyrosin" in a trade name, the sorts of paints are of five colors; black, gray, brown, green and silver, in addition to these, beige paint for a radiant heating system is used. It seems these all paints are the heat resisting paints in a kind of silicon resin. A standard of the coating method is double coatings with a painting brush, the back surface of specimen is all coated with "Pyrosin Black" to be easily heated by absorbing the radiation energy from a heater.

The measurements on the nonmetallic specimens were performed at the

experimental conditions that temperatures of specimens as well as black body were each of 100°C, 200°C, 300°C and 400°C, the changes of temperature during the experiments were  $\pm 1\%$  of specimen temperature and  $\pm 0.5\%$  of black body temperature, furthermore, room temperature was 20~21°C and relative humidity 45~53%.

#### 4. Experimental Results and Considerations

The measured results are shown in Fig. 5 and Fig. 6, on the scratched rough aluminum surfaces covered with the vacuum deposit of aluminum and on the scratched rough brass surfaces respectively. The measured values of the surface roughness with a roughness tester are shown in Table 1.

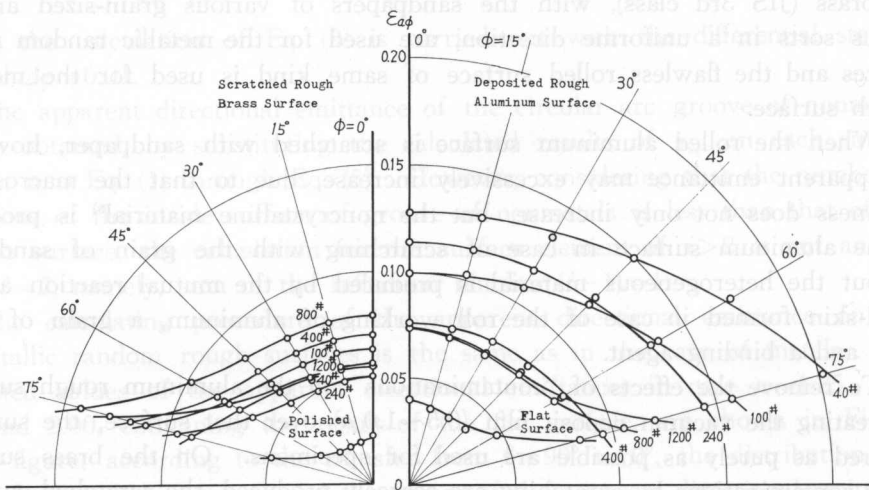


Fig. 6. Apparent directional emittances of the scratched rough brass surfaces (measured values).

Fig. 5. Apparent directional Emittances of the deposited rough aluminum surfaces (measured values).

Although the measured values of the apparent normal emittance on the aluminum rough surfaces covered with the vacuum deposit appear to be in proportion to the measured values of the roughness, except for the specimen scratched with the 100 # sandpaper, it does not seem that only the dimension of roughness yields these results. That is, in comparison between an absolute value and a graphic form of the apparent directional emittance, the measured value for a flat smooth surface is similar to that of the calculated result of the flat surface in case  $n=50$ , the measurements for the rough surfaces scratched with the 1200 #, the 800 # and the 400 # sandpapers are similar to the calculations for  $\hat{\gamma}=75\sim 90^\circ$ ,  $60\sim 75^\circ$  and  $45\sim 60^\circ$  in case  $n=30$  respectively, the measurements of the rough surfaces scratched with the 240 # and the 100 # are similar to the calculations for  $\hat{\gamma}=45\sim 60^\circ$  and  $60\sim 75^\circ$  in case  $n=20$  respectively and the measured value for a rough surface scratched with the 40 # is similar to the calculated value for  $\hat{\gamma}=60\sim 75^\circ$  in case  $n=15\sim 20$ .



These results will be explained by the conception that a graphic form of the apparent directional emittance is determined by an opening-ratio (ratio of pitch to depth of a groove or a cavity) which is obtained from the roughness analysis described in the next chapter, and an absolute value of the emittance is determined by refraction index which indicates a degree of "contaminations" of the surface. In this place, it will be considered that the contaminations consist of (1) chemical change of the surface, (2) physical change of the surface, such as the cohesive heterogeneous materials, and (3) microroughness of the surface.

**Table 1.** Measured Values of Roughness and Roughness-Shapes of the Metallic Specimens

Specimens		Ha ( $\mu$ )	Hrms ( $\mu$ )	Hmax ( $\mu$ )	Distribution Shape of Roughness	
					Directional Emittance; $\hat{\tau}$	Roughness Curve; $\hat{\tau}$
Deposited Rough Surface of Aluminum	40 # AA	5.0	5.5	27.0	60~75°	~75°
	100 # AA	2.8	3.4	14.0	60~75°	~75°
	240 # AA	1.9	2.2	10.0	45~60°	60~75°
	400 # AA	1.0	1.1	5.3	45~60°	60~75°
	800 # CC	0.6	0.6	2.0	60~75°	75~90°
	1200 # CC	0.5	0.5	1.3	75~90°	75~90°
	Smooth	0.5	0.5	0.4	~90°	~90°
Scratched Rough Surface of Brass	40 # AA	2.2	2.3	11.4	~60°	60~75°
	100 # AA	1.3	1.3	6.0	75~90°	~75°
	240 # CC	1.0	1.1	4.6	75~90°	~75°
	400 # CC	0.8	0.8	2.1	75~90°	75~90°
	800 # CC	0.6	0.7	0.7	75~90°	75~90°
	1200 # CC	0.6	0.6	0.7	~90°	~90°
	Polish	0.5	0.6	0.4	~90°	~90°

AA: Alumina Grain Sandpaper    CC: Carborundum Grain Sandpaper

It is shown that, also on the scratched rough surfaces of brass the same tendency as in the aluminum results is observed, and if the absolute value and the graphic form of the measured values are compared with those of the calculated values, the normal emittance has no connection with the measured roughness. That is, the measured value of a polished surface is similar to the calculated value of a flat surface in case  $n=90$ , the measured value of a rough surface scratched with 1200 # sandpaper is similar to the calculated value of a flat surface for  $n=30$ , the measurements of the rough surfaces with the 800 #, the 400 # and the 100 # are similar to the calculations for  $\hat{\tau}=75\sim90^\circ$ ,  $n=30$ , the measured value of a rough surface with the 240 # is similar to the calculated value for  $\hat{\tau}=75\sim90^\circ$ ,  $n=40$ , and the measured value of a rough surface with the 40 # is similar to the calculated value for  $\hat{\tau}=60^\circ$ ,  $n=40$ . These correspond also to the analytical results of roughness curves as a whole. In Table 1, are shown the

values of  $\hat{\tau}$  taken from the absolute value and the graphic form in comparison between the measurements and the calculations of the apparent directional emittance, as well as the values converted into  $\hat{\tau}$  the average opening-ratio on the analytical results of the roughness curves.

The measured values of the painted smooth surfaces and the painted rough surfaces are indicated in Fig. 7. The values of the apparent directional emittances of each painted smooth surface are nearly constant up to  $\phi=45^\circ$ , and decrease steeply over about  $60^\circ$ . This tendency and absolute value of the directional emittance agree well with Fresnel's formula, and from the fact, it seems the refraction index  $n$  of the painted specimen has a value within the region

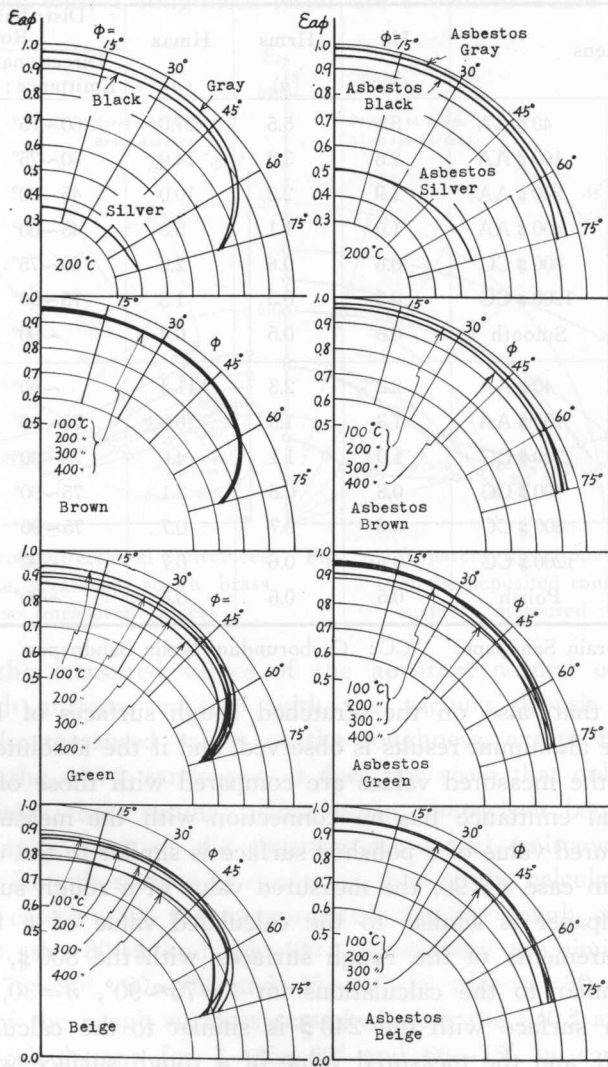


Fig. 7. Apparent directional emittances of the flat smooth and the rough painted surfaces (measured values).

of 1.50~2.50 reversibly, except for silver paint. Though a value of the normal emittance of silver paint is less than that of other paints, in proportion to the increment of  $\phi$  the directional emittance increase slightly and a few metallic property appears. It seems that a reason for these is in the fact that silver paint consists of aluminum powder for main contents of pigment. The value of the apparent directional emittance of the painted rough surface increases more than that of the painted smooth surface; the tendency of increment of each paint, is remarkable in direction to the large directional angle  $\phi$ , therefore, the graphic form of the apparent directional emittance approaches to semi-circular shape. This tendency and absolute value of the measurements agree well with those of the calculated values for  $\hat{\tau}=45^\circ$  of the nonmetallic random rough surface. The tendency of the measured value of the directional emittance on a silver painted rough surface decreases slightly in a rate of the expansion of tails of the curve and is similar as that in case of the metallic rough surfaces.

In Table 2, are shown the film thickness of the painted smooth surface and the painted rough surface, the measured value with a roughness tester, the value of  $\hat{\tau}$  taken from the absolute value and the graphic form of the directional emittances in comparison between the measurements and the calculations,

**Table 2.** Measured Values of Coating Film Thickness, Roughness and Roughness-Shapes of the Painted Specimens

Property of Paint Surface Paint Specimens		Painted Flat Smooth Surface					
		Thickness of Coated Film (mm)	Surface Roughness			Distribution Shape of Roughness	
			Ha ( $\mu$ )	Hrms ( $\mu$ )	Hmax ( $\mu$ )	Directional Emittance; $\hat{\tau}$	Roughness Curve; $\hat{\tau}$
Black	0.19	3.6	3.9	5.4	90°~Flat Surface	75~90°	
Gray	0.07	1.3	1.4	3.5			
Brown	0.09	2.1	2.3	5.4			
Green	0.11	1.3	1.4	2.7			
Beige	0.07	1.2	1.3	4.3			
Silver	0.07	1.5	1.7	4.0	—	—	

Property of Paint Surface Paint Specimens		Painted Rough Surface					
		Thickness of Coated Film (mm)	Surface Roughness			Distribution Shape of Roughness	
			Ha ( $\mu$ )	Hrms ( $\mu$ )	Hmax ( $\mu$ )	Directional Emittance; $\hat{\tau}$	Roughness Curve; $\hat{\tau}$
Black	0.46	13	12	34	~45°	45~60°	
Gray	0.41	13	14	31			
Brown	0.30	10	12	28			
Green	0.44	13	14	22			
Beige	0.36	13	14	27			
Silver	0.28	11	12	50	—	—	

as well as the value converted into  $\hat{\gamma}$  the average opening-ratio obtained from the analysis of the roughness curve.

The phenomenon of increment of the normal emittance on the painted rough surfaces is explained by Sparrow's theory<sup>9)</sup>, assuming the irregularity of the rough surface composes of the spherical cavities with various opening-ratios, but the explanation for increment of the directional emittance is difficult.

### 5. Analysis of Roughness Curve

In case of the analysis of the roughness curves recorded with a roughness tester (Kosaka SE-4; probe radius  $5 \mu$ , needle pressure 0.4 g), as shown in Fig. 8, the dimension and the shape of roughness will be defined by expressions of the roughness pitch (P) and the opening-ratio (P/Hm). On the roughness curves, the cavity narrower than a radius of probe is cut off and the microroughness which is considerably smaller than the root mean square roughness  $H_{rms}$  is omitted from the subject of analysis.

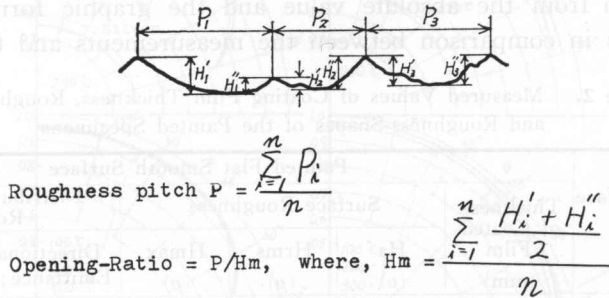


Fig. 8. Analysis of roughness curve.

By such method are carried out the roughness curve analyses of the deposited rough aluminum surfaces and the scratched rough brass surfaces, the analytical results are shown by the number of the distribution frequencies in Fig. 9 (a) and (b). A feature of the surface roughness can be observed from these diagrams, and by converting the opening-ratio of the roughness curve into the value of  $\gamma$ , the measured values can be compared with the calculated values through the  $\hat{\gamma}$ . That is, the roughness pitches of the deposited aluminum surfaces become large in proportion to the grain size of the sandpaper except for the flat smooth surface and the opening-ratio is largest on the flat smooth surfaces and smallest on the rough surfaces scratched with the 240 # or the 400 #. These facts mean that on the rough surfaces scratched with the 240 # or the 400 # distribute the comparative deep cavities of  $\hat{\gamma} = 60 \sim 75^\circ$ , and on the other rough surfaces, the open shallow cavities of  $\hat{\gamma} = 75 \sim 90^\circ$ , and these values of  $\hat{\gamma}$  agree with those taken from the graphic form of the directional emittance (Table 1). Why the roughness pitches on the flat smooth surfaces are measured in large values, will be that the microroughness is neglected without the detection and but the swellings by the roll working are measured.

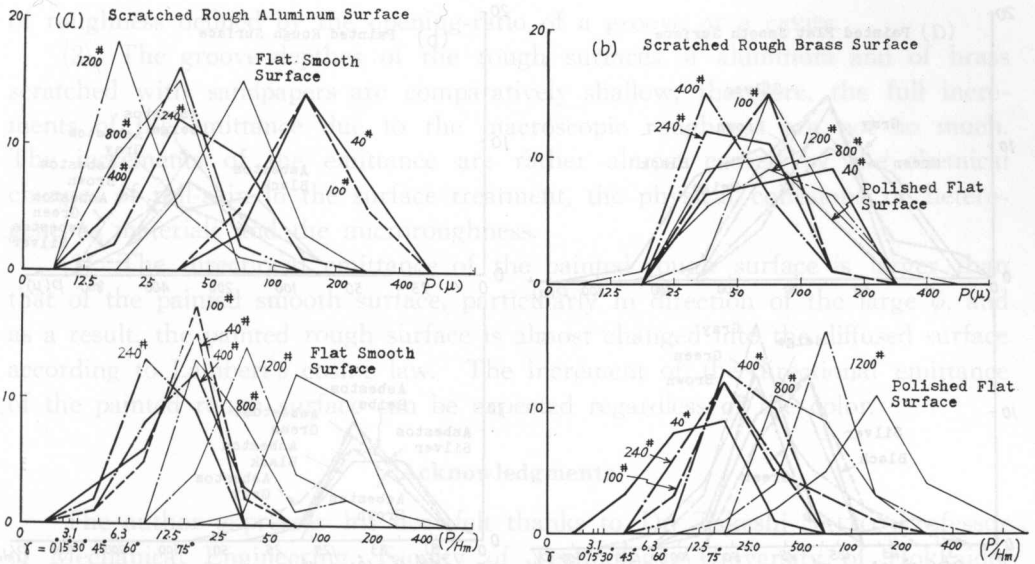


Fig. 9. Distribution frequencies of roughness pitches ( $P$ ) and opening-ratios of the metallic specimens ( $P/H_m$ ).

- (a) Scratched rough aluminum surfaces.
- (b) Scratched rough brass surfaces.

On the scratched brass surface, the roughness pitches of the rough surfaces scratched with the 400 # and the 240 # are of small values and the roughness pitches of the other surfaces are large. However, an opening-ratio of the rough surface with the 40 # is smallest of  $\hat{\gamma} = 60 \sim 75^\circ$ , those of the other surfaces are values of  $\hat{\gamma} = 75 \sim 90^\circ$  and those of the polished surface and the rough surface with the 1200 # are nearly equal to the value of the flat smooth surface, these tendencies appear on the graphic forms of the directional emittances, and an agreement between both is obtained (Table 1).

The analytical results of roughness curves on the flat surface coated with only paint and the rough surface coated with asbestos mixture paint are shown in Fig. 10 (a) and (b). In these diagrams, it is indicated that the roughness pitches on the painted flat surface are small and those of the painted rough surface are large as a whole, but on the opening-ratio of the painted rough surfaces distribute a number of the large pitched and moreover deep cavities reversibly. The opening-ratios of the painted flat surface and the painted rough surfaces correspond to  $\hat{\gamma} = 75 \sim 90^\circ$  and  $\hat{\gamma} = 30 \sim 60^\circ$  respectively, and so concerning both of the tendency and the absolute value, the measured values of the directional emittance for each  $\hat{\gamma}$  agree well with the calculated values.

The dimension of the opening of circular arc groove which is considered as an analytical model is equivalent to the pitch of roughness curves of the specimen, and though on the analysis, it is assumed that the dimension of the opening of the circular arc groove is larger than the wavelength of radiation, this assumption is almost satisfied also on the specimens. Namely, in the

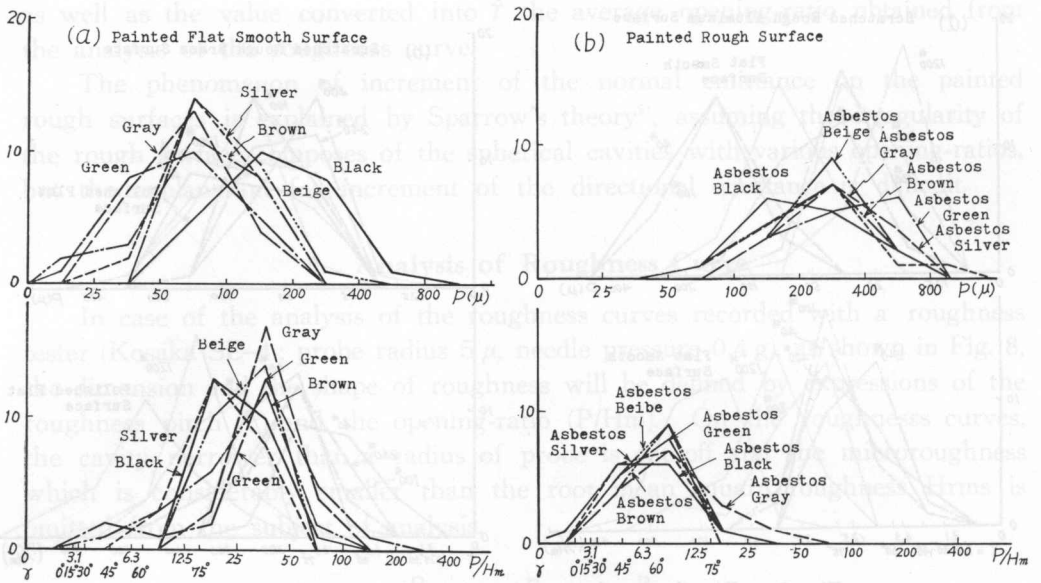


Fig. 10. Distribution frequencies of roughness pitches ( $P$ ) and opening-ratios of the nonmetallic specimens ( $P/H_m$ ).

- (a) Painted flat smooth surfaces coated with only paint.  
 (b) Painted rough surfaces coated with asbestos mixture paint.

temperature region  $100\sim 400^\circ\text{C}$ ,  $70\sim 85\%$  of the radiation energy distributes between  $3\sim 15\mu$  wavelength, on the other hand, the greater part of the roughness pitches of individual specimen is larger than  $12.5\mu$  except for a few part of overlapped region, so that it may be regarded that the dimension of the roughness pitch is almost larger than the wavelength.

## 6. Conclusions

Assuming that the random rough surfaces of metals and nonmetals could be modeled as the rough surfaces composed of various sorts of the circular arc grooves, the theoretical analyses of the apparent directional emittances of these surfaces were performed.

The analytical results of the directional emittances on the metallic materials were compared with the measured values on the rough surfaces of aluminum and of brass scratched with sandpapers, the results of the directional emittances on nonmetallic materials were compared with the measured values on the rough surfaces coated with various kinds of paints, and an agreement between both was obtained.

The other points which have been made clear in this study are as follows:

- (1) It seems that the directional emittances of the metallic and the nonmetallic rough surfaces are directly of no relation to the dimensions of roughness measured with a roughness tester;  $H_a$ ,  $H_{rms}$  or  $H_{max}$ , but relate to the shape

of roughness defined by the opening-ratio of a groove or a cavity.

(2) The groove depths of the rough surfaces of aluminum and of brass scratched with sandpapers are comparatively shallow, therefore, the full increments of the emittance due to the macroscopic roughness are not so much. The increments of the emittance are rather almost caused by the chemical changes of roll-skin in the surface treatment, the physical cohesions of heterogeneous materials and the microroughness.

(3) The directional emittance of the painted rough surface is larger than that of the painted smooth surface, particularly in direction of the large  $\phi$ , and as a result, the painted rough surface is almost changed into the diffused surface according to Lambert's cosine law. The increment of the directional emittance of the painted rough surface can be expected regardless of the color.

### Acknowledgments

The author expresses his heartfelt thanks to Dr. Takeshi SAITO, Professor of Mechanical Engineering, Faculty of Technology, University of Hokkaido, for his kind directions in this study, and to Mr. Hiromu BABA, Assistant of Kitami Institute of Technology, for his joint efforts in the numerical calculation.

### References

- 1) Schmidt, E.,: *Forschung Gebiete Ing.*, **6**, 175 (1935-7~8).
- 2) Hase, V. R.,: *Zeitschr. f. Techn. Physik*, **3**, 146 (1932).
- 3) Kanayama, K.,: *Trans. JSME.* (in contribution).
- 4) Jakob, M.,: *Heat Transfer*, **1**, 47 (1964), Jhon Wiley & Sons.
- 5) Kanayama, K.,: *Trans. JSME.*, **37**, 299, 1378 (1971-7).
- 6) Katto, Y.,: *Trans. JSME.*, **22**, 122, 693 (1956-10).
- 7) Hasunuma, H.,: *J. Japan Soci. Precision Engg.*, **22**, 4, 131 (1956-4).
- 8) *Handbook of Aluminum Machining Technique*, 519 (1970), Nikkan Kogyo Shinbunsha.
- 9) Sparrow, E. M.,: *Trans. ASME.*, **84**, 2, Ser. C, 188 (1962-2).